

M. KOPERNIK\*, M. PIETRZYK\*

## 2D NUMERICAL SIMULATION OF ELASTO-PLASTIC DEFORMATION OF THIN HARD COATING SYSTEMS IN DEEP NANOINDENTATION TEST WITH SHARP INDENTER

### NUMERYCZNA SYMULACJA 2D ODKSZTAŁCENIA SPREŻYSTO-PLASTYCZNEGO UKŁADU CIENKICH TWARDYCH POWŁOK W TEŚCIE WCISKANIA WGLĘBNIKA O OSTREJ KOŃCÓWCE

In this paper hard coating systems are considered as an investigated material and their behaviour under static loading is analyzed. Experimental nanoindentation test is one of the most demanding in obtaining mechanical properties of thin films and such test is simulated using finite element method (FEM). Numerical simulation follows the experiment and it gives satisfying results in many technical and research areas. Distributions of computing values using FEM models for multilayer systems are presented in the paper. Capabilities and difficulties in simulation of thin hard coating systems are described, that is an important step to achieve further purpose, which is a complete and precise numerical analysis of properties of hard coating systems in deep nanoindentation test.

*Keywords:* hard coating system, FEM, nanoindentation test, plastic deformation

W niniejszej pracy badano układy twardych powłok i ich zachowanie pod wpływem obciążeń statycznych. Próba wciskania wgłębnika jest jednym z najważniejszych doświadczeń przeprowadzanych dla cienkich warstw i jej numeryczna symulacja została przeprowadzona przy użyciu metody elementów skończonych. Przedstawiono wyniki w postaci rozkładów intensywności naprężeń, odkształceń, a także krzywych postaci siła-przemieszczenie obliczanych dla każdego etapu odkształcenia. Dodatkowo opisano możliwości stworzonego modelu numerycznego i trudności związane z modelowaniem powłok. Praca stanowi krok w kierunku otrzymania własności twardych powłok na podstawie wyników symulacji testu wciskania wgłębnika.

## 1. Introduction

Thin hard coating systems have main features of functionally graded materials (FGM). These materials have new interesting properties and/or functions that cannot be achieved by conventional homogeneous materials. Due to very small scale and contrasting physical properties in adjacent, very thin layers, graded nanomaterials are challenging in laboratory and numerical tests. Significant numerical difficulties rise from thickness of layers, which produces necessity of mesh regeneration on very small thickness. Also multimaterial character of simulation is not easy to be computed. Generating correct FEM model for multilayer system will be very important, numerical task. Mentioned problems boil down to connecting different types of numerical solutions simultaneously. Thus, the first objective of this paper is creation of the direct numerical model for nanoindentation

test and inverse analysis. Using this model, the second purpose is numerical simulation of deformation in deep nanoindentation test and estimation its preciseness and efficiency.

FEM is helpful in solving problems of design of nanocoatings by anticipating behaviour of these materials. Many coatings and surface treatments have been developed to enhance component performance and, increasingly, coating architectures are becoming more complex as multilayer, superlattice and graded coating systems become widely available. There are so many potential coating variants, that it is almost impossible to test all the possibilities to optimise their performance. The need for predictive models is increasing, but model development has generally lagged behind the introduction of new coatings [1]. Therefore, following Authors earlier research [2] FEM is applied in this paper to modelling the deep nanoindentation tests and to predict specified

\* DEPARTMENT OF APPLIED COMPUTER SCIENCE AND MODELLING, FACULTY OF METALS ENGINEERING AND INDUSTRIAL COMPUTER SCIENCE, AGH UNIVERSITY OF SCIENCE AND TECHNOLOGY, 30-059 KRAKÓW, AL. MICKIEWICZA 30, POLAND

propagation, location and value of plastic deformation. Deep nanoindentation with sharp indenter can be simulated only when remeshing problem is solved in the program. Forge 2 commercial code with remeshing procedure implemented is used in this work to obtain better quality of computing results in die/specimen contact region. Numerical graph representing force versus depth is another important, designing information, which is an output from the program. This graph is used in further analysis to get calculated hardness and indentation modulus. The objective of the paper is solving various numerical problems connected with simulation of nanoindentation test to create a possibility of prediction of the depth versus force curves. The predictions are not compared with experimental data at this stage of the project.

Inverse analysis is the perspective application of the model. Material properties can be obtained after correct inverse analysis of the experimental data. Then, parameters from the inverse analysis will be set into FEM program and create a possibility to get results for thin multilayer system [3] comparable to experimental ones in nanoindentation tests. Many Authors [4] raise this problem, but they get numerical results only in shallow range of depth, because of problems with remeshing, which causes difficulties. In paper [5] Authors show only weakly deformed meshes and do not explore further this subject. Elements in weakly deformed meshes do not need new mesh generation during computation process, but output results cannot be compared to the experimental ones.

## 2. Materials

### 2.1. Basis of thin hard coating systems

In this paper thin hard coating systems are investigated and it is commented upon meaning of designing ability, which is achieved in predicting material behaviour and properties in nanoindentation test. The main designing rules used in producing these systems come from tribology and are set into material in manufacturing process. Such rules are visible in products, which are tested in the paper, because they are tribological coatings of third generation. Tribological hard nanocoatings of the third generation, eg. (Ti, Zr)N, (Ti, Cr)N, (Ti, Al, V)N, (Ti, Al, Si)N are usually investigated in experimental nanoindentation tests. The idea of multilayer system manufacturing derives from tribological conclusions, which confirm that mixing elastic-plastic, thin coatings on base (substrate) give definite, expecting effects. For tribological coatings, the mechanical response to contact is particularly important if performance has to be understood. In paper [1] Authors briefly review developments in numerical simulation and extend recent modelling developments in an energy-based predictive FEM model for the hardness and Young's modulus of a coated system. The model can be applied to a single layer of multilayer coatings successfully. Model predictions can be improved by considering the through-thickness fracture behaviour of the coating.

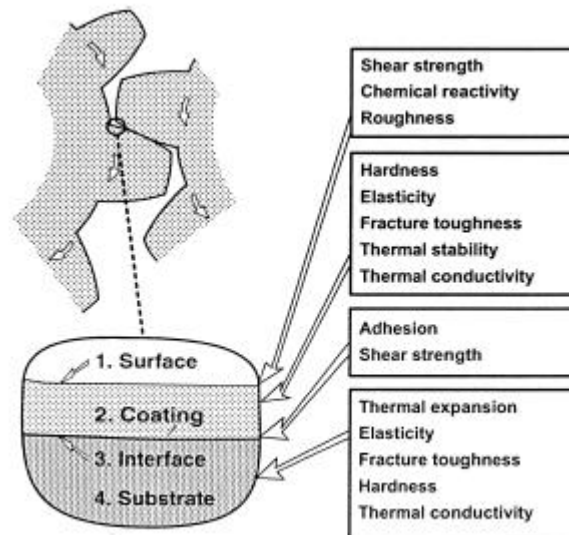


Fig. 1. Tribologically important properties in different zones of the coated surface [6]

Some practical applications of tribology principles in this subject are risen in [6]. The Authors show that thin hard coatings on a soft substrate generate lower stresses in the coating and at the coating/substrate interface compared to thick hard coatings with the same deflection. According to [6] a multilayer coating with alternate hard and soft layers can allow deflection to occur under load without yielding of the hard layers. They effectively slide over each other, with shear occurring in the soft layer. The pattern of shear is illustrated by the line through the film, which is initially straight in the unloaded condition. Many important, tribological problems are solved in designing and manufacturing such system, some of them are presented in figure 1.

## 2.2. Specimen description

Hard coating systems are analysed during modelling. They consist of titanium nitride basis, thin mixed elastic-plastic multilayers deposited on elastic substrate. Two systems are considered, like:

- system 1 – MT-CVD (medium temperature chemical vapour deposition) three, thin material layers on carbide,
- system 2 – PVD (physical vapour deposition) eleven, thin material layers.

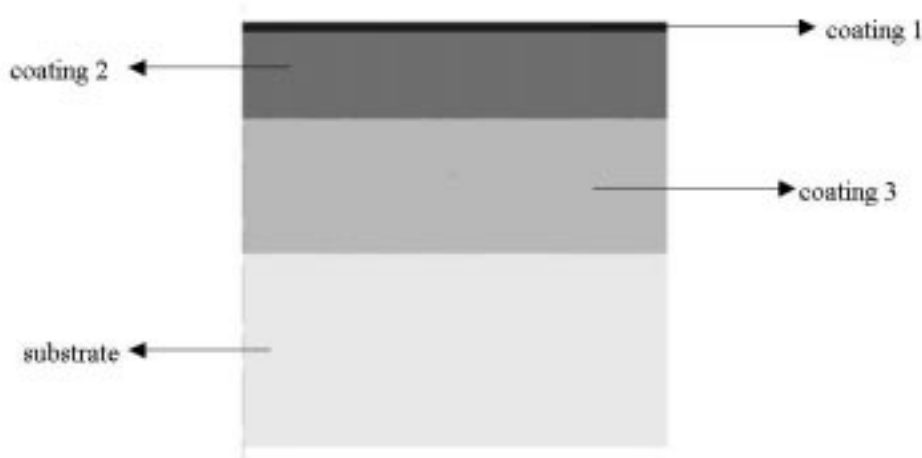


Fig. 2. System 1 is shown as three different coatings deposited on elastic substrate

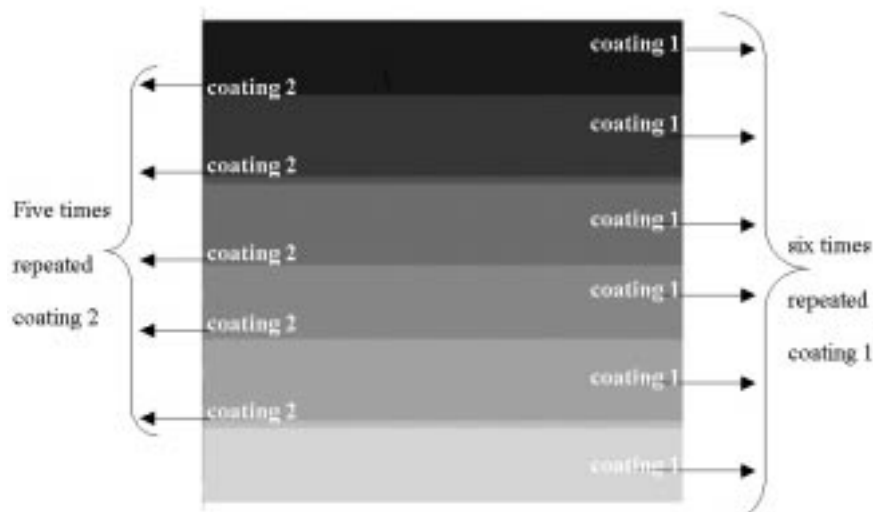


Fig. 3. System 2 is shown as two different coatings deposited periodically, coating 2 is repeated five times and coating 1 is repeated six times, respectively. Coating 2 is very thin

Systems 1 and 2 are presented in figures 3 and 4, where length scale is respected. Each coating shows material layer used in material system. Systems 1 and 2 are technical materials.

### 2.3. Material properties

Properties of used layers are presented in tables 1 and 2.

TABLE 1

System 1. Elastic and plastic properties of layers used in system 1

Material	coating 1 [7]	coating 2 [8]	coating 3 [9, 10]	substrate <a href="http://www.matweb.com">http://www.matweb.com</a>
Elastic properties				
Elastic modulus $E$ , GPa	616	370	535	683
Poisson ratio $\nu$	0.25	0.22	0.25	0.3
Plastic properties				
Yield strength $\sigma_0$ , MPa	5000	3000		
Strain hardening $A$ , GPa	50			
Specimen width, $\mu\text{m}$	22.0			

TABLE 2

System 2. Elastic and plastic properties of layers used in system 2

Material	coating 1 <a href="http://www.matweb.com">http://www.matweb.com</a>	coating 2 [7]
Elastic properties		
Elastic modulus $E$ , GPa	380	616
Poisson ratio $\nu$	0.177	0.25
Plastic properties		
Yield strength $\sigma_0$ , MPa		5000
Strain hardening $A$ , GPa		50
Specimen width, $\mu\text{m}$	22.0	

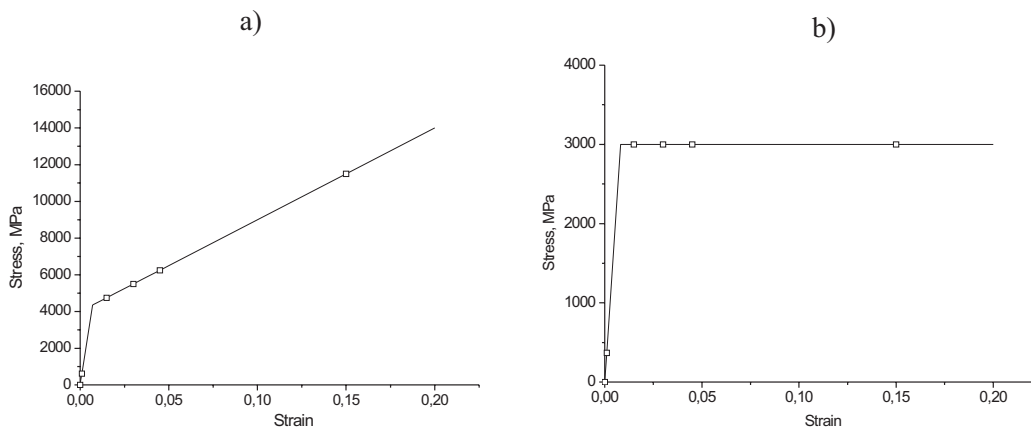


Fig. 4. Stress-strain curves for: a) coating 1 (system 1) and coating 2 (system 2), b) coating 2 (system 1)

According to properties set in tables 1 and 2 for the coating 1 in system 1 and for the coating 2 in system 2 the linear hardening law for flow stress description is used (figure 4a) and introduced in chapter 2.4:

$$\sigma_f = \sigma_0 + A\varepsilon_i = \sqrt{3}K_0 + (\sqrt{3}K_0a)\varepsilon_i, \quad (1)$$

where:  $A = 50000$  MPa,  $\sigma_0 = 4000$  MPa.

In equation (1)  $\varepsilon_i$  represents effective strain. According to properties set in table 1 for the coating 2 in system 1 the elastic-ideal plastic law for flow stress description is used (figure 4b) and also introduced in chapter 2.4:

$$\sigma_f = \sigma_0 = \sqrt{3}K_0, \quad (2)$$

where:  $\sigma_0 = 3000$  MPa.

The FEM model of the specimen is 2D axisymmetric. Thickness of each layer is smaller than its width, but the details are not revealed by the manufacturer.

#### 2.4. Material rheological models in FEM program

The Forge 2 program is designed for forging simulation in various conditions. This FEM based computing code solves numerical problems related to large deformations, which occur in mesh elements during the process. Initial mesh is being rebuilt, when it is necessary (mesh elements are too deformed) and it is called remeshing operation. Since considered case needs new mesh generation in many computing steps, the Forge 2 code is chosen. Some numerical problems arise and they are related to very small thickness of coating 2 in system 2. Due to remeshing procedure, more than one node (the best number of nodes is three) must be generated on a very small distance (equal to thickness of coating 2). During remeshing procedure new elements are created and more nodes are required.

The description of the rheology of the material in FORGE2<sup>®</sup> is based on the Norton-Hoff flow rule written in the following tensorial form:

$$\sigma_i = 2K(T, \varepsilon_i, \dots) \left( \sqrt{3}\dot{\varepsilon}_i \right)^{m-1} \dot{\varepsilon} \quad (3)$$

This relation links the deviatoric stress tensor  $\sigma_i$  to the strain rate tensor  $\dot{\varepsilon}$  through the consistency  $K(T, \varepsilon_i, \dots)$  and the sensitivity to the strain rate  $m$ . The theoretical behaviour corresponding to the value  $m = 1$  also called Newtonian behaviour, can also be integrated in FORGE2<sup>®</sup>. In this case, the set of equations describing the problem of mechanical equilibrium is linear. In equation (3)  $T$  is temperature,  $\varepsilon_i$  is effective strain and  $\dot{\varepsilon}_i$  is effective strain rate.

Elasto-viscoplastic flow rule is used, in which plastic stress is related to strain hardening, strain rate  $\dot{\varepsilon}$  and the temperature following the equation:

$$\sigma_i = \sqrt{3}^{(1+m)} K_0 (1 + a\varepsilon_i) \exp\left(\frac{\beta}{T}\right) \dot{\varepsilon}_i^m \quad (4)$$

where:  $K_0$  – consistency term,  $a$  – coefficient,  $\beta$  – thermal dependency,  $m$  – strain rate sensitivity.

According to specified material properties, which are presented in previous chapter (tables 1 and 2, equations (1) and (2), and figure 4), both materials are not sensitive to the temperature and to the strain rate ( $m = 0$  and  $\beta = 0$ ). The values of remaining parameters in equation (4) are given in table 3.

TABLE 3

Parameters in equation (4)

Parameter	$a$	$K_0$ , MPa
System 1		
Coating 1	12.5	2309.4
Coating 2	0	1732.05
System 2		
Coating 2	12.5	2309.4

The remaining material layers are elastic and only elastic properties are required in material models. As it was mentioned the description of the material rheological behaviour in FORGE 2 is based on the elastic-plastic laws. It signifies basically that the following assumption for the material is true: at every moment, it is possible to separate the instantaneous deformation in the elastic reversible part  $\varepsilon_e$  and plastic irreversible part  $\varepsilon_p$ . In a tensorial form, this hypothesis is written as follows:

$$\varepsilon = \varepsilon_p + \varepsilon_e. \quad (5)$$

#### Elastic behaviour

Part of the material deformation is represented by a reversible elastic behaviour, which is idealized through the linear elasticity law in the following form:

$$\varepsilon_e = \frac{1+\nu}{E}\sigma_i + \frac{3\nu}{E}pI, \quad (6)$$

where  $I$ : unit tensor

In the above relationship,  $\varepsilon_e$  represents the elastic small strains tensor,  $\sigma_i$  is the stress tensor. Hydrostatic pressure  $p$  is given by the formula:

$$p = -\frac{1}{3}\text{trace}(\sigma_i) \quad (7)$$

The parameters defining the material elastic behaviour are Young modulus  $E$  and the Poisson ratio  $\nu$ . These parameters are supposed to be constant and they are entered in the data file. Pressure calculated by the FORGE 2 program is equal to negative value of the average stress, which is a term used in mechanical and plastic

processing. This relationship is expressed as: pressure = average stress.

### Plastic behaviour

When the material behaviour is considered as elasto-plastic, the description of the variables related to the plastic part of the deformation is based on the H u b e r - M i s e s criterion. A simplified way of describing this criterion is:

- if  $\sigma_i = \sigma_{eq}$  : plastic deformation occurs  
 if  $\sigma_i < \sigma_{eq}$  : elastic deformation occurs

where:  $\sigma_{eq}$  is equivalent stress (effective stress) and is defined as one of the stress tensor invariants with the following expression:

$$\sigma_{eq} = \frac{1}{2} [ (\sigma_{XX} - \sigma_{YY})^2 + (\sigma_{YY} - \sigma_{ZZ})^2 + (\sigma_{ZZ} - \sigma_{XX})^2 ] , \quad (8)$$

where:  $\sigma_{XX}$ ,  $\sigma_{YY}$ ,  $\sigma_{ZZ}$  are main stresses on Cartesian directions.

Effective strain  $\varepsilon_i$  is defined by equation:

$$\varepsilon_i = \int_0^t \sqrt{\frac{2}{3}} \varepsilon^T \dot{\varepsilon} dt, \quad (9)$$

where:  $\dot{\varepsilon}$  – plastic strain rate tensor.

### 3. Standard laboratory test

The International Organization for Standardization (ISO) has produced an international standard ISO 14577 [11], which can be applied to instrumented indentation test.

The determination of properties on the basis of this test is divided into three ranges:

- Macro range:  $2 \text{ N} < F < 30 \text{ kN}$ ,
- Micro range:  $2 \text{ N} > F; h > 200 \text{ nm}$ ,
- Nano range:  $h < 200 \text{ nm}$ .

The indentation test can be either under force  $F$  or under depth  $h$  control. Experimental nanoindentation test gives the following mechanical properties:

- hardness,
- elastic modulus,
- creep resistance,
- temperature-dependent properties.

No other technique provides information about both the elastic and plastic properties of thin films. Nanoindentation test, which is used as example for numerical simulations in this work, is performed in load-controlled mode using a Nano Test System [11]. Indentations are 20-cycle load-controlled load-partial unload experiments

from 1 mN to 20 mN maximum load. An uncoated substrate wafer is tested for comparison. The data are interpreted and calculated with the O l i v e r and P h a r r method [12] and repeated load-partial unload experiments are performed on each sample. The O l i v e r - P h a r r method is used in depth sensing indentation machines with Berkovich indenter [10]. Berkovich is deformable, elastic diamond, tip radius is assumed to 100-150 nm, effective cone angle is  $140.64^\circ$  [13].

### 4. Numerical test

Conditions for numerical simulation of nanoindentation test are similar to those in laboratory test, but a geometry simplification is made (specimen cross-section is taken in simulation). Berkovich shape deformable probe (tip radius 150 nm) is set to specimen surface. Such tool – Berkovich shape deformable probe, is simulated as a semi-cone cross-section – it moves into specimen and is set as a constant velocity press in program settings. The numerical indentation test is under depth control. Knowing velocity and displacement as an input data, force versus depth is calculated, as well as pressure, equivalent strain and stress distributions. Applying 2D and axisymmetric model [14] is an often made simplification (advantage – shortening of computing time), which is also introduced in the present work. Such model is purposeful and it does not cause a lost of important information. Number of indentations steps is fixed to 10 (system 1) and 20 (system 2). Deformed mesh from previous computing step is set into next step as an initial mesh. This operation is made as well as mesh regeneration (remeshing procedure), the last one occurs when elements are too distorted. Remeshing procedure solves numerical problems related to large deformations, which occur in mesh elements during process. Initial mesh is being rebuilt, when it is necessary (mesh elements are too distorted) and it is called remeshing operation. Considered case needs new mesh generation in many computing steps and it was a reason that this program is chosen. Some numerical problems arise and they are related to very small thickness of coating 2 in system 2. On a very small distance (equal to thickness of coating 2) more than one node (the best number of nodes is three) must be generated, because of remeshing procedure. During remeshing procedure new elements are created and more nodes are required.

After each loading step, elastic unloading is made and after this computing step, new loading is set to deformed specimen surface. There is a difference between experimental test and numerical one. In experiment, only partial unloading is made and in simulation there is a total unload, whole specimen is able to springback.

Adjusting tooling is done manually after each step that is why every load step starts exactly from the specimen surface. Moving die is a deformable tool and has its own mesh, but its deformation is not presented in figures in this paper, because of this work's aim, which is focused on specimen.

Coulomb friction law is used in simulations. Friction coefficient  $\mu$  in die-specimen contact region is equal to 0.12. In experiment friction is an unwanted parameter, but there is no possibility to get such ideal conditions in deformation process.

## 5. Numerical model

### 5.1. Numerical model and results of hard coating system 1

Numerical model for hard coating system 1 is as follows:

- number of nodes: 1350,
- number of triangular elements: 2530.

Multilayer specimen discretization for FEM analysis is presented in figure 5. Initial, numerical, axisymmetric model is used in the test and it is shown as mesh before the test with deformable die – Berkovich shape, deformable die (figure 5a). In die/specimen contact region, an enlargement is made, because it is the most deformed zone. Local mesh refinement in the program

leads to fine mesh in nodal contact region. Correct mesh in such area yields good results, because of mesh regeneration necessity.

Whole deformed die/specimen contact region and box showing mesh refinement in contact region are presented in figures 6a – 6c. Deformation depth extends quite far, so there is a necessity of remeshing, what is successfully achieved by the program.

The largest strain values are obtained in die/surface region (figures 6j – 6l) and remain there during the whole test, therefore only this region of interest is displayed in figure 6. Distributions of computed values are calculated after unloading, so they have plastic character and remain in elastic-plastic layers – in this case in the upper layers. Strain distributions change during test and finally received wing-like shape, which slightly spreads out over a coating 1/coating 2 contact area (boundary region).

Pressure distributions have similar character in the whole test, but the maximum value increases and in the last computing step reaches the maximum value in the tip of Berkovich shape indenter. In the range of maximum pressure distributions occur minimum pressure zones (figures 6e and 6f), which have surface character.

Effective stress distributions (figures 6g – 6i) are like pressure ones. There are not meaningful minimum zones inside effective stress distributions observed in the applied scale. However, analysis of numerical results shows that one minimum of effective stress zone occurs at the coating 1 and coating 2 boundary.

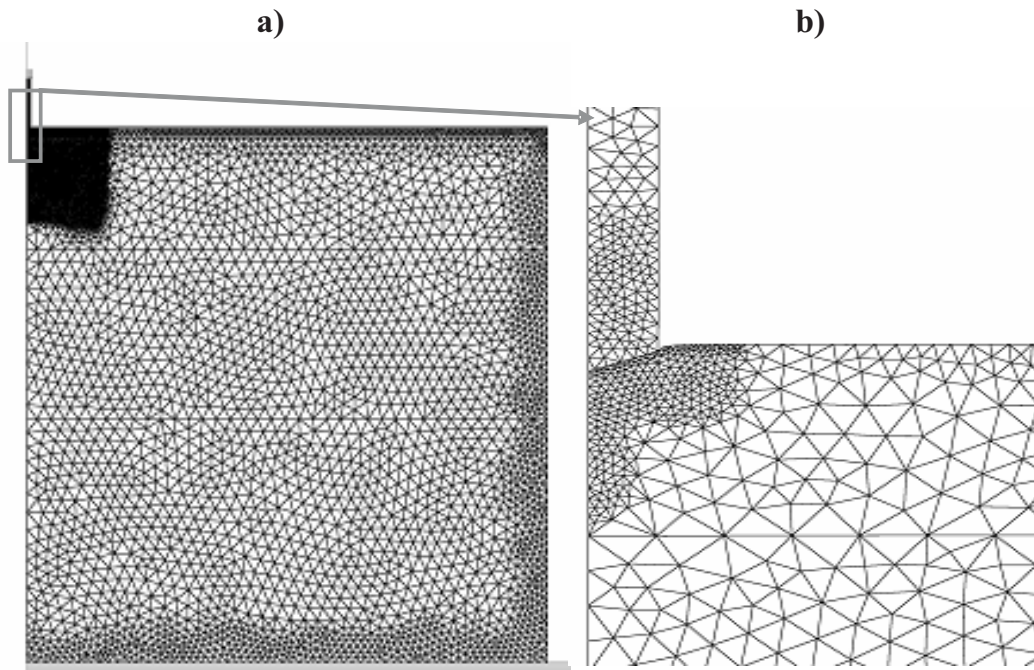


Fig. 5. a) Not deformed specimen and die, and b) weakly deformed contact region between specimen and moving die

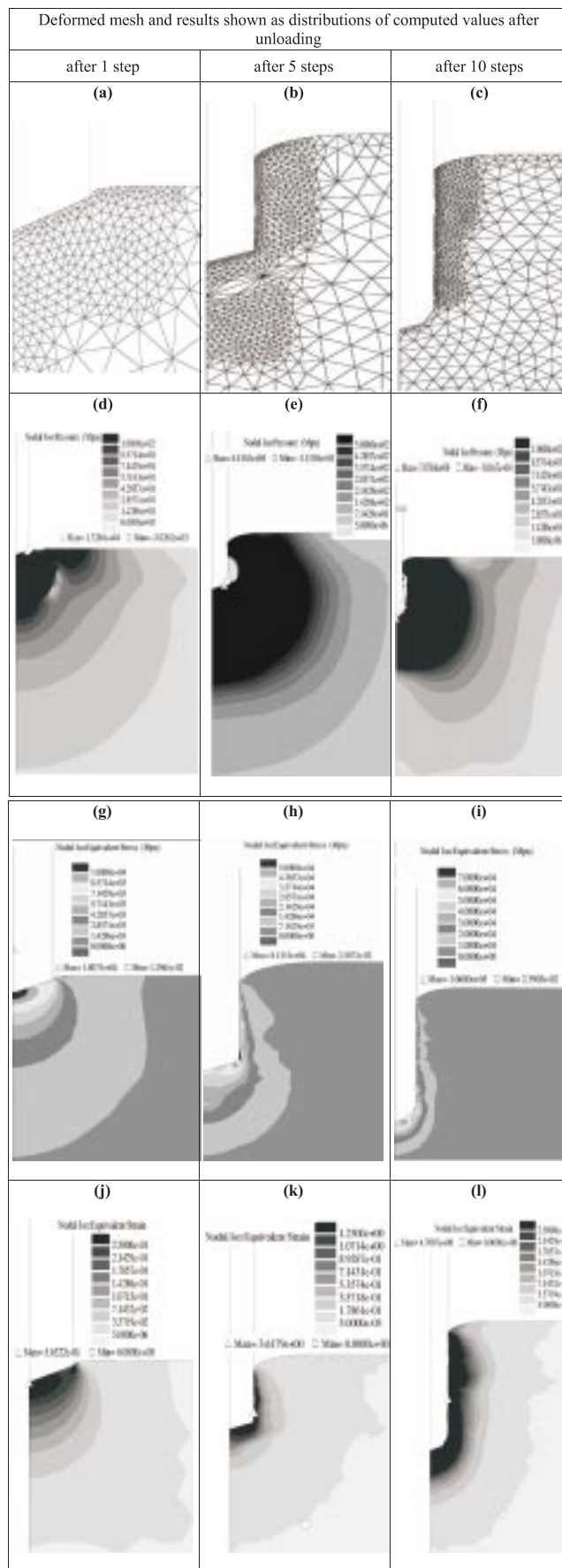


Fig. 6. Deformed mesh and distributions of computed values



Force versus depth curve is the most important in an experimental nanoindentation test [11], which allows to get stiffness, the Martens hardness and reduced elastic modulus. As well as in experiment, in numerical modelling of nanoindentation test force versus depth graph is obtained (figure 7). Predicted relationship is similar to the experimental one – curve character is kept, but in the applied program it is impossible to get partial unloading curve. Complete unloading process is done in the program, but load output data is not generated during this period. Further modelling tasks should provide unloading part of each curve and such operation is possible to reach, only when process control will be modified. Graph (figure 7) is composed of ten curves (loading curves), but the unloading curves are not presented. Unloading part of each curve is necessary, when stiffness and reduced elastic modulus are to be calculated.

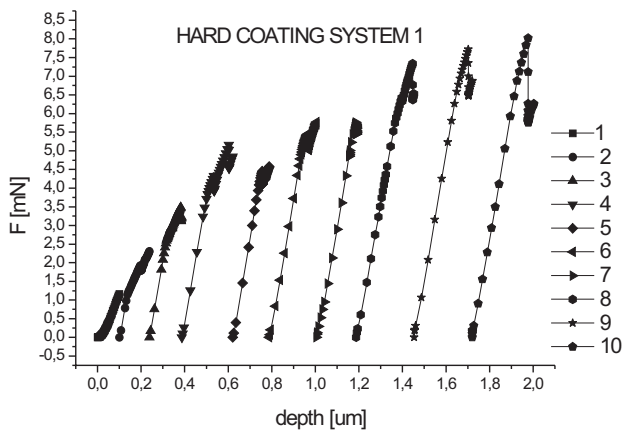


Fig. 7. Force versus depth graph for hard coating system 1

## 5.2. Numerical model and results for hard coating system 2

Numerical model for hard coating system 2 is set as follows:

- number of nodes: 5836,
- number of triangular elements: 11335.

Multilayer specimen discretization for FEM analysis is presented in figure 8. Initial, numerical, axisymmetric

model is used in the test and it is shown in figure 8a as mesh at the beginning of the test. Berkovich shape, deformable, upper die can be distinguished. Enlargement is made in die/specimen contact region in figure 8b. Local mesh refinement in program leads to fine mesh in contact region. Correct mesh in such area provides good results, because of mesh regeneration necessity.

Whole deformed die/specimen contact region and local mesh refinement are presented in figures 9a – 9c. Deformation depth extends not very far, but in spite of such numerical convenience, there is a necessity of remeshing, especially in the thin coating 2 area, what is successfully achieved by the program.

The largest strain value is obtained in the first coating 2 (figures 9j – 9l) and remains there during the whole test, therefore, this region of interest is displayed in figure 9, especially in figures 9a – 9c. Distributions of presented values are calculated after unloading, so they have plastic character and remain in elastic-plastic layers – in this case in the alternating thin coating 2 and under Berkovich shape indenter tip. Shape of strain distributions almost does not change during the test and finally reaches maximum value in the first coating 2.

Pressure distributions (figures 9d – 9f) have similar character in the whole test, but the maximum pressure value increases and in the last computing step reaches the maximum value in the tip of Berkovich shape indenter. Range of maximum pressure in distributions occurs in upper coating 2 and under Berkovich shape indenter tip and is situated on loading direction.

Effective stress distributions (figures 9g – 9i) are similar to pressure ones, but are not exactly the same. There are not meaningful differences observed between shape of pressure and effective stress distribution. Material layer boundary – coating 2/ coating 1 is seen as a horizontal disturbance in effective stress distribution in corresponding thickness level – between coating 1 and coating 2.

Upper part of equivalent stress distributions is slightly different from the pressure one. Effective stress distribution has jug-like shape and the range of maximum value is also present in surface part of the specimen.

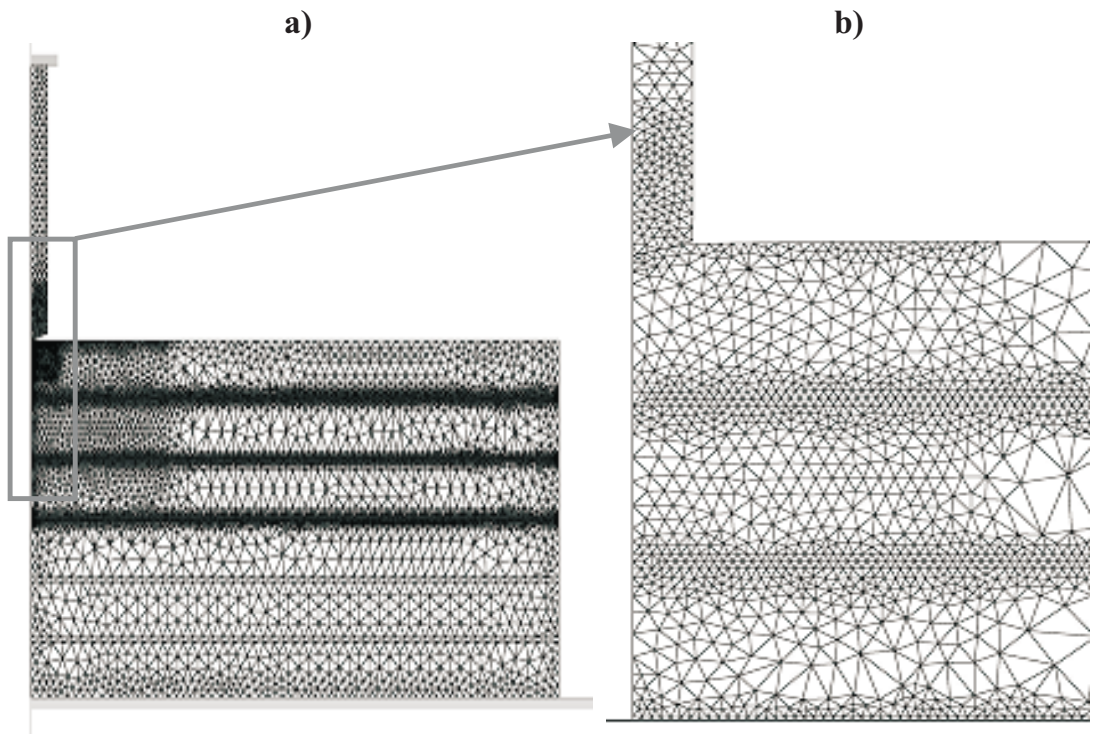
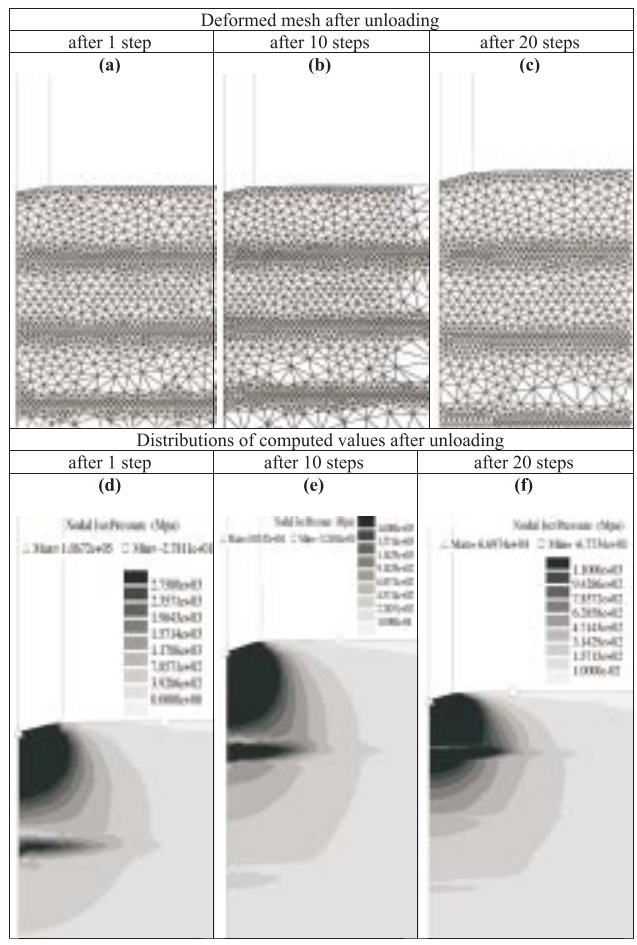


Fig. 8. a) No deformed specimen and dies, and b) weakly deformed contact region between specimen and moving, deformable die



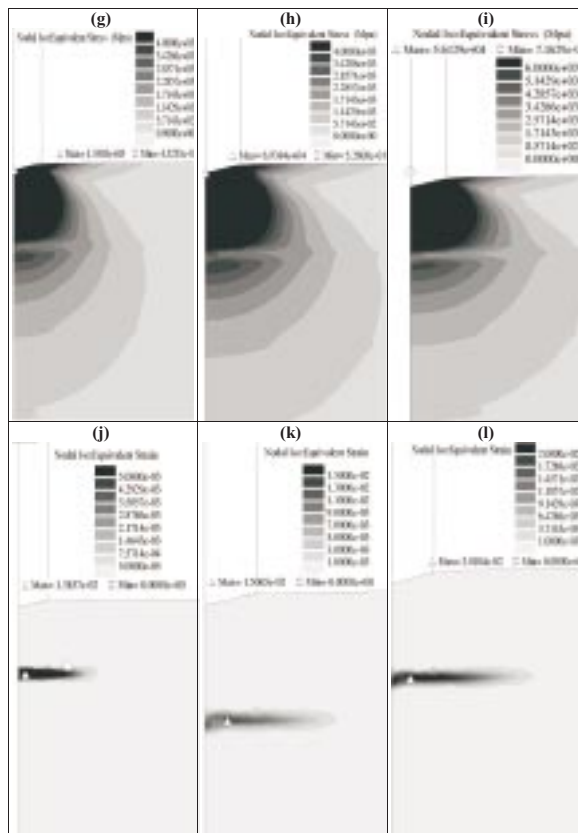


Fig. 9. Deformed mesh and distributions of computed values

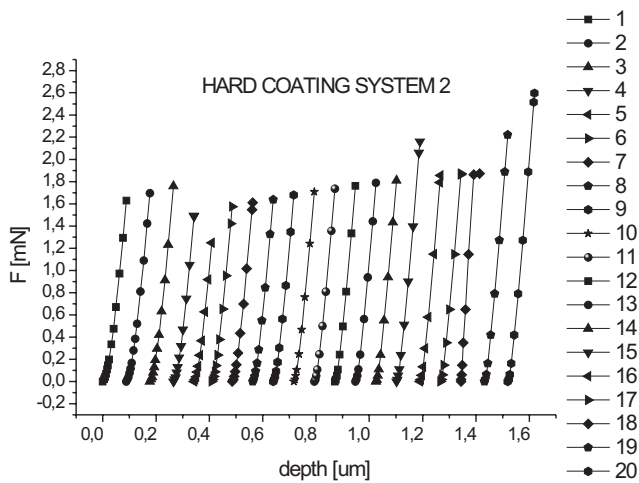


Fig. 10. Force versus depth graph for hard coating system 2

As it has been mentioned before, force versus depth curve is the most important in an experimental nanoindentation test, which allows to get further knowledge about examined material. As well as in experiment, in numerical simulation of deep nanoindentation test force versus depth graph is obtained (figure 10) for hard coating system 2. It looks similar to the experimental graph – curve character is kept, but in used program it is im-

possible to get partial unloading curve during this period. Complete unloading process is simulated by the program, but load output data is not generated. Further modelling tasks should provide data to obtain unloading part of each of twenty curves, as it was mentioned in chapter 5.1.

## 6. Conclusions and final comments

Numerical simulations of deep nanoindentation test were carried out for the two different hard coating systems. FEM models for two multilayer systems were generated and their correctness was verified during simulations, which have repeatable character. Also remeshing problem was solved properly and created models were able to reconstruct real, experimental conditions. Some approximations were made, but in an acceptable field. Results of simulations seem to be helpful in determining location, propagation and value of plastic deformation in thin hard coating systems. Developed models proved their good predictive capability and will be further used as direct problem models in the inverse analysis of nanoindentation test [15, 16].

Differences between numerical and experimental tests, especially in control process of loading, are re-

moved when goal function is defined for the hardness. Computing hardness using presented here numerical models is possible, because values of depth can be directly measured on FEM mesh and unloading curve is not necessary to obtain values of depth, as it is required in experimental test. Values of depth are set in equations of hardness. Such procedure was successfully realized in paper [16] by the Authors.

Summarizing, inverse analysis leads to better material models and precise material mechanical properties. It can be very efficient, numerical instrument in analysis of thin, hard nanocoatings and designing their new systems.

#### Acknowledgements

Financial assistance of the MNiSzW, project no. N50713632/3962, is acknowledged.

#### REFERENCES

- [1] S.J. Bull, E.G. Berasetegui, T.F. Page, Modelling of the indentation response of coatings and surface treatments, *Wear* **256**, 857-866 (2004).
- [2] M. Kopernik, M. Pietrzyk, A. Żmudzki, Numerical simulation of elastic-plastic deformation of thin hard coating systems in nano – impact test, *Computer Methods in Materials Science* **6**, 150-160 (2006).
- [3] M. Kopernik, M. Pietrzyk, Possibilities of modelling of graded nanomaterials, *Proc. 13<sup>th</sup> Konf. Kom-PlasTech*, ed., Szeliga, D., Pietrzyk, M., Kusiak, J., Szczawnica, 291-296 (2006).
- [4] M. Lichinchi, C. Lenardi, J. Haupt, R. Vitali, Simulation of Berkovich nanoindentation experiments on thin films using finite element method, *Thin Solid Films* **333**, 278-286 (1998).
- [5] D. Ma, K. Xu, J. He, Numerical simulation for determining the mechanical properties of thin metal films using depth-sensing indentation technique, *Thin Solid Films* **323**, 183-187 (1998).
- [6] K. Holmberg, A. Matthews, H. Ronkainen, Contact mechanism and surface design, *Tribology International* **31**, 107-120 (1998).
- [7] X. Cai, H. Banger, Finite-element analysis of the interface influence on hardness measurements of thin films, *Surface and Coatings* **81**, 240-255 (1996).
- [8] <http://www.matweb.com>
- [9] A.T. Santhanam, D.T. Quinto, G.P. Grab, Comparison of the steel-milling performance of carbide inserts with the MTCVD and PVD TiCN coatings, *Int. J. of Refractory Metals and Hard Materials* **14**, 31-40 (1996).
- [10] A.R. Franco, G. Pintaúde, A. Sinatora, C.E. Pinedo, A.P. Tschiptschin, The use of a Vickers indenter in depth sensing indentation for measuring elastic modulus and Vickers hardness, *Materials Research* **7**, 483-491 (2004).
- [11] B.D. Beake, S.P. Lau, Nanotribological and nanomechanical properties of 5-80 nm tetrahedral amorphous carbon films on silicon, *Diamond and Related Materials* **14**, 1535-1542 (2005).
- [12] C. Oliver, G.M. Pharr, An improved technique for determining hardness and elastic modulus using load and displacement sensing indentation experiment, *J. Mater. Res.* **7**, 1564-1583 (1992).
- [13] A.J. Fischer-Cripps, *Nanoindentation*, Springer-Verlag p6 ISBN 0-387-95394-9 (2002).
- [14] M. Paszyński, M. Kopernik, Ł. Madej, M. Pietrzyk, Automatic hp adaptivity to improve accuracy of modeling of heat transport and linear elasticity problems, *J. Machine Eng.* **6**, 73-82 (2006).
- [15] M. Kopernik, M. Pietrzyk, Evaluation of possibilities and perspectives of application of nanomaterial hard coatings, *Computer Methods in Materials Science* **6**, 42-63 (2006).
- [16] M. Kopernik, M. Pietrzyk, Rheological model and mechanical properties of hard nanocoatings in numerical nanoindentation test, 10<sup>th</sup> Esaform conference on material forming, Zaragoza, Spain, AIP conference proceedings, 907, 659-664 (2007).